

Division of Engineering
BROWN UNIVERSITY
PROVIDENCE, R. I.

A7CRL 582

AF-4561/11

ON THE IMPLICATIONS OF ELECTRON DIFFUSION
THROUGH THE HYPERSONIC SHOCK FRONT
BY
LEWIS WETZEL

Wetzel
1-17-72
1-17-72

COPYRIGHT

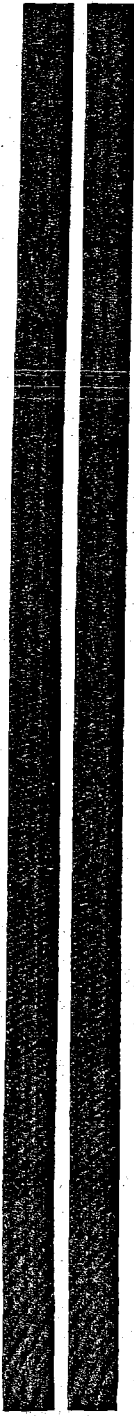
AD 262746

Air Force Cambridge Research Laboratories
Office of Aerospace Research
Contract A7 19(604)-4561
Scientific Report A7-4561/11

AF-4561/11

TECHNICAL LIBRARY
U S ARMY ORDNANCE
ABERDEEN PROVING GROUND, MD.
OEDBG-TL

May 1961



ON THE IMPLICATIONS OF ELECTRON DIFFUSION
THROUGH A HYPERSONIC SHOCK FRONT

By

Lewis Wetzel

Scientific Report AF 4561/11

DIVISION OF ENGINEERING

BROWN UNIVERSITY

PROVIDENCE, RHODE ISLAND

May 1961

Contract Monitor: Dr. Werner W. Gerbes

"The research reported in this document has been sponsored in part by the Electronics Research Directorate of the Air Force Cambridge Research Laboratories, Office of Aerospace Research, and by the Office of Naval Research and the David Taylor Model Basin. The publication of this report does not necessarily constitute approval by the Air Force of the findings or conclusions contained herein."

Contract title: Research Directed toward the study of Radiation of Electromagnetic Waves

(Contract number: AF 19(604)-4561)

Best Available Copy

TECHNICAL LIBRARY
U. S. ARMY ORDNANCE
ABERDEEN PROVING GROUND, MD.
ORDBG-TL

20060223384



"Requests for additional copies by Agencies of the Department of Defense, their contractors, and other Government agencies should be directed to the:

ARMED SERVICES TECHNICAL INFORMATION AGENCY
ARLINGTON HALL STATION
ARLINGTON 12, VIRGINIA"

"All other persons and organizations should apply to the:

U. S. DEPARTMENT OF COMMERCE
OFFICE OF TECHNICAL SERVICES
WASHINGTON 25, D.C."

Table of Contents

<u>Section</u>	<u>Page</u>
Abstract	ii
I. Introduction	1
II. The Precursor Distribution	6
III. Some Implications of the Transient Behavior	14
A. Comparison of the theory with some experimental results	15
B. Effect of the transient on the scattering of electromagnetic waves	19
1. Low-Frequencies	22
2. High-Frequencies	23
3. Intermediate-Frequencies	27
IV. Summary and Conclusions	32
References	35

Abstract

Recent experiments have disclosed electrical effects well ahead of an advancing shock front. Certain of these effects have been attributed to the diffusion of electrons through the shock front from the ionized region behind it. In this report, the diffusion hypothesis is examined in terms of a simple heuristic model, in which the diffusion is assumed to take place from a plane electron source moving with the shock velocity. The predictions of this model are shown to be generally consistent with the available experimental evidence. It is further shown that the transient behavior of the precursor electron distribution is capable of increasing the Doppler shift of an electromagnetic wave reflected from the shock. Although the transient decays rapidly after the creation of the shock, there are conditions under which it should last long enough to allow an experimental check of this effect.

I. Introduction

Recent experiments in shock tubes have disclosed the presence of a variety of electrical effects in the region well ahead of the advancing shock front.⁽¹⁻⁴⁾ Several hypotheses have been proposed to explain the existence of these effects, but no one of them alone can account for all of the observations. The observations themselves, which consist of signals recorded from probes placed along the shock tube, may be classified according to the apparent velocity of the precursor signal. Some of these signals appear to propagate with effectively infinite velocities, and are presumably caused by photo-effects from the delayed luminosity.⁽²⁾ Others propagate with velocities of the order of the shock speed, and have been attributed to the diffusion of electrons upstream through the shock front.⁽¹⁾ Signals in the latter class have been observed even when the delayed luminosity did not appear⁽²⁾, and seem to have been detected only when the shock was formed in one of the noble gases. It is significant that the noble gases exhibit a pronounced Ramsauer effect for electron energies corresponding to the temperatures generally existing in the equilibrium region behind a hypersonic shock front. The recent discovery of transient "double fronts" in small bore electric shock tubes⁽⁵⁾ might be interpreted as further evidence of precursor electron activity, although this behavior has been ascribed to the high-energy electrons from the energizing electric arc⁽⁶⁾, rather than to the ionization created by the shock.

At present the diffusion hypothesis rests almost entirely on somewhat meager experimental evidence, the complex character of the shock front region

making an adequate theoretical investigation extremely difficult. We will not attempt such an investigation here. Instead, we will review the current picture of how ionization takes place, then speculate briefly on some aspects of the diffusion problem. In so doing, it is hoped that the simple heuristic model on which the conclusions of this report are based will be made plausible.

It is reasonable to ask first about the electron and ion densities which would appear if diffusion were ignored. According to Petschek and Byron⁽⁷⁾ (among others), the ionization process can be roughly divided into two stages. The shock-heated gas reaches thermal equilibrium directly behind the shock front, and as one moves downstream, a certain amount of initial ionization takes place as a result of atom-atom and atom-impurity collisions. As the electron density grows, electron-atom collisions take over as the primary ionizing mechanism, and the gas is fairly quickly ionized to the equilibrium level. Thus we have the picture of the electron (and ion) concentration starting from zero at the shock front, rising slowly behind the shock front for a while, then increasing rapidly to the equilibrium level. Although the details will depend on the type of gas, the shock speed, the impurity concentration, etc., the general behavior of the plasma concentration may be represented by the following picture:

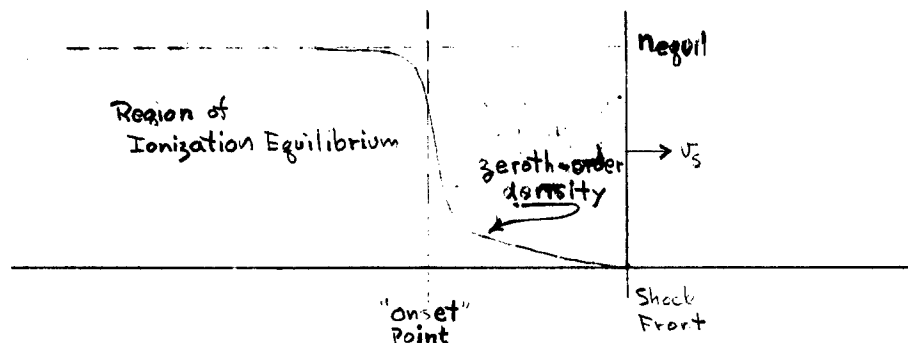


Fig. 1

This does not, of course, represent the steady-state electron concentration, since diffusion has been ignored. The electrons have much larger diffusion coefficients than the ions, so they will tend to diffuse out of the plasma, leaving the ions behind. The electrostatic space-charge fields arising from this charge separation will retard the flow of electrons, but we cannot predict to what extent and in what manner without first producing a convincing solution for the diffusion problem associated with the ionization variations on which Fig. 1 is based. It is just here that the theory is stalled. Electron flow in the presence of space-charge effects has been considered in other contexts, however, and it will be helpful to speculate from the point of view of a few of these results.

We observe, first of all, that the zeroth-order concentrations change from very small values directly behind the shock front to very large values in the region of ionization equilibrium behind the "onset point". Now the two extremes of electron diffusion out of a plasma concentration may be characterized by the ambipolar and the free diffusion coefficients, corresponding respectively to high and low plasma densities. Where there is a large variation of plasma density, as in the case being considered here, one may expect a transition between the ambipolar and free diffusion regimes, and this transition may affect the character of the entire diffusion process in a complicated way. For example, Allis and Rose⁽⁸⁾ have considered transition diffusion in the case of a microwave discharge in a cavity, and have obtained good agreement between theory and experiment. Although diffusion into an open region, as through a shock front, introduces additional complications, the above suggests that the diffusion of electrons from the low-density tail

of the distribution shown in Fig. 1 might be governed by a coefficient approaching that for free diffusion. It is important that this possibility should exist, because if electrons are to succeed in outrunning the shock to the extent suggested by the experimental data, there must be a reservoir of electrons with large diffusion coefficients available behind the shock front. An objection can be raised here that the electrons created by the ionization processes in the onset region are left with relatively low energies, and they lack sufficient time to come into equilibrium with the shock-heated gas. Therefore even the free diffusion coefficient will be too small to account for the observed precursor distributions.

We may refer here to an analogous situation encountered in the low-voltage arc. In this device it is found that a stable arc in a noble gas can be maintained at voltages which are less than half the excitation potential for the gas involved. Probe measurements disclose the existence of a positive ion concentration in the center of the arc which results in an accelerating field from cathode to space-charge, and a strong decelerating field from space-charge to anode. Electrons from the cathode are therefore accelerated to the excitation potential at the center of the arc, but having excited the gas atoms, are left with virtually zero energy. The magnitude of the observed arc current, however, requires that a large fraction of these electrons must overcome a potential barrier of about 7v to reach the anode. The question: where do they get the necessary energy? This question was successfully answered by Druyvesteyn,⁽⁹⁾ who showed that the exhausted electrons gain energy from those electrons which arrive from the cathode, but have failed to excite

any of the gas atoms. The relaxation time for this equilibration is only about one mean free time between electron-electron collisions, which is very small compared with the large times required for a low energy electron to reach equilibrium with the hot neutral gas. If we imagine some such process to be operative in heating the cool electrons in the onset region directly behind the shock front, we are left with the problem of finding a source of hot electrons to do the job. This is not hard, because the only source of hot electrons lies behind the onset point, in the region of ionization equilibrium. The supply of electrons here is copious and energetic, so there now exists the possibility of "thermionic emission" from this region. What is meant by this is that electrons from the high-energy tail of the Maxwell distribution move across the potential barrier, which is produced by charge separation, and mingle with the low energy electrons in the onset region. In this way the electrons close to the shock front could be given sufficient energy to diffuse upstream.

The considerations of the last two paragraphs suggest a simple model from which certain implications of electron diffusion may be found. If a "reservoir" of diffusible electrons is to exist behind the shock front, then we must be able to define a steady-state density, n_p , for the electrons contained in it. (The reader is cautioned not to take the term "reservoir" too literally.) Since the probability is low, on a random-walk basis, that an electron far behind the front will contribute to the precursor distribution, we may assume that this reservoir is located in a narrow region of width d , directly behind the shock front. In order to maintain the steady-state

density n_p in this region, the shock must generate new electrons at the rate $n_p v_s/d$ per unit volume to replace those that are left behind as the shock moves along. If we consider a one-dimensional shock, then we approximate this picture by collapsing the precursor reservoir into a plane electron source of strength $(n_p v_s/d) \times (d) = n_p v_s$, located at the shock front itself. We will denote the temperature of this source by T_p . In this way, then, we have replaced the real, but intractable, situation by a fictitious model consisting of a plane source moving with the shock velocity v_s and characterized by two parameters, n_p and T_p , into which are lumped the unknowns of the problem. If accurate measurements could be made of the precursor distribution, these parameters could be determined empirically.

In the next section the precursor distribution predicted by this model will be derived. Following this, it will be shown that if a reasonable interpretation of the available measurements is allowed, the time-dependence of the predicted precursor behavior is consistent with the experimental results. Finally, it is suggested that under suitable conditions, an electromagnetic wave incident upon a shock front might experience a transient enhancement of its Doppler shift.

II. The Precursor Distribution

Before examining the transient behavior of the precursor electron distribution, let us obtain the steady-state distribution by means of an elementary argument. Consider a shock-based reference system in which the shock front is fixed and the driven gas streams through it with velocity

v_s , as in Fig. 2 below:

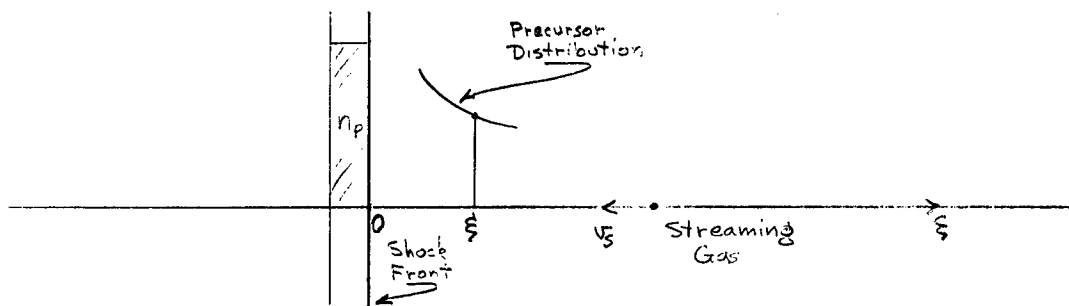


Fig. 2

Under steady-state conditions in this system, the diffusing electrons must arrange themselves into a distribution of such a form that the drift velocity due to the concentration gradient is equal and opposite to the velocity of the streaming gas. This is expressed by the equation

$$-\frac{kT_p}{m\nu_c} \frac{1}{n} \frac{dn}{d\xi} = v_s \quad (1)$$

where ξ is the distance upstream measured from the shock front, T_p is the electron temperature, m is the mass of the electron and ν_c is the collision frequency for electrons of temperature T_p in the neutral gas. (The electrostatic self-field of the distribution has been ignored in view of the relatively low electron densities expected.) Since it is being assumed that these electrons emerge from a region maintained at a steady-state density n_p , Eq. 1 may be solved as

$$n(\xi) = n_p e^{-\frac{v_s}{D}\xi} \quad (2)$$

where $D = v_o^2/3\nu_c$ ($v_o^2 = 3kT_p/m$) is the coefficient for free diffusion of the electrons in the neutral gas. Weymann claims that this ξ -dependence

can be verified if T_p is taken as the equilibrium temperature behind the shock front.⁽⁴⁾ If, in addition, an absolute measurement of electron density can be made for some value of ξ , then n_p can be determined. This is a model parameter, however, and has no particular physical significance.

In order to obtain the transient behavior, the plane-source model described at the end of the last section will be used. We consider a one-dimensional shock which is created at time $t = 0$ at the origin of coordinates, $x = 0$. Thus one might have in mind a shock tube in which a diaphragm at $x = 0$ is burst at $t = 0$. We will be interested in laboratory measurements of precursor effects, hence in the electron density existing at a fixed point x at a time t before the shock front has arrived. Figure 3 represents a "snapshot" of the advancing shock front, showing its position relative to the point of observation at the time, t , of observation.

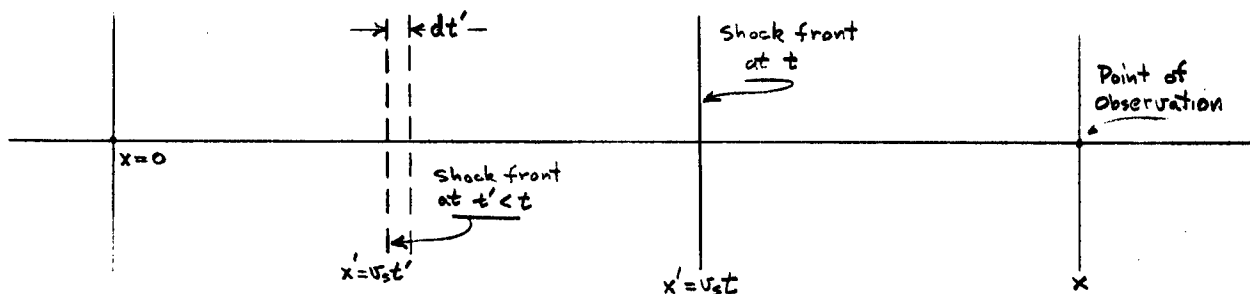


Fig. 3

Observe, however, that the precursor electrons have been diffusing out of the shock front over the entire time interval from 0 to t , thus the density at (x, t) represents an accumulation of electrons created at earlier times.

This accumulation process may be described analytically as follows. If we let x' be the position of the shock front at a time $t' < t$, (see Fig. 3), then in the time interval dt' the source at the front produces $n_p v_s dt'$ potential precursor electrons. Some of these diffuse toward x , and their contribution to the precursor density at x at the later time t can be written

$$dn(x,t; x',t') = \frac{n_p v_s}{\sqrt{4\pi D}} \frac{e^{-\frac{(x-x')^2}{4D(t-t')}}}{\sqrt{t-t'}} dt', \quad (3)$$

where D is the diffusion coefficient defined earlier. The total accumulation at (x,t) is found by putting $x' = v_s t'$ and integrating Eq. 3 from 0 to t ,

$$n(x,t) = \frac{n_p v_s}{\sqrt{4\pi D}} \int_0^t e^{-\frac{(x-v_s t')^2}{4D(t-t')}} \frac{dt'}{\sqrt{t-t'}}. \quad (4)$$

The integral can be evaluated by converting it into the form of a convolution of two functions. In terms of the variable $\tau = t - t'$, Eq. 4 becomes

$$n(x,t) = \frac{n_p v_s}{\sqrt{4\pi D}} \int_0^t e^{-\frac{[x-v_s(t-\tau)]^2}{4D\tau}} \frac{d\tau}{\sqrt{\tau}}. \quad (5)$$

Multiplying out the exponent,

$$-\frac{[x-v_s(t-\tau)]^2}{4D\tau} = -\frac{(x-v_s t)^2}{4D\tau} - \frac{v_s}{2D} (x - \frac{1}{2} v_s t) + \frac{v_s^2}{4D} (\tau - t),$$

and using the notation $(x - v_s t) = \xi$, we may write (5) as

$$n(x,t) = \frac{\eta p v_s}{\sqrt{4\pi D}} e^{-\frac{v_s}{2D}(x - \frac{1}{2}v_s t)} \int_0^t \frac{e^{-\frac{v_s^2}{4D}\tau^2}}{\sqrt{\tau}} e^{\frac{v_s^2}{4D}(t-\tau)} d\tau. \quad (6)$$

The integral in (6) is now in the form of a convolution,

$$f * g = \int_0^t f(\tau) g(t-\tau) d\tau, \quad (7)$$

which may be expressed as

$$f * g = \mathcal{L}^{-1}[\mathcal{F}\mathcal{G}], \quad (8)$$

where \mathcal{F} and \mathcal{G} are the respective Laplace Transforms of f and g , and \mathcal{L}^{-1} denotes the inverse transform. The transforms of the two functions in the integrand of (6) may be found in almost any table of Laplace Transforms to be

$$\mathcal{F} = \mathcal{L}\left[\tau^{-\frac{1}{2}} e^{-\frac{v_s^2}{4D}\tau}\right] = \sqrt{\frac{\pi}{D}} q^{-\frac{1}{2}} e^{-\frac{q}{8D}} \quad (9)$$

$$\mathcal{G} = \mathcal{L}\left[e^{\frac{v_s^2}{4D}\tau}\right] = (p - \alpha)^{-1},$$

where $q = (p/D)^{\frac{1}{2}}$ and $\alpha = v_s^2/4D$. Thus, if we let I be the integral in Eq. 6, we may write

$$I = \sqrt{\frac{\pi}{D}} \mathcal{L}^{-1}\left[\frac{e^{-\frac{q}{8D}}}{q(p-\alpha)}\right]. \quad (10)$$

Performing the inversion, one obtains,

$$I = \frac{\sqrt{\pi D}}{v_s} e^{\frac{v_s^2}{4D} t} \left\{ e^{-\frac{v_s}{2D} \xi} \operatorname{erfc} \left(\frac{\xi - v_s t}{\sqrt{4Dt}} \right) - e^{+\frac{v_s}{2D} \xi} \operatorname{erfc} \left(\frac{\xi + v_s t}{\sqrt{4Dt}} \right) \right\}, \quad (11)$$

which, when substituted into Eq. 6, yields $n(x,t)$ in the form:

$$n(x,t) = \frac{1}{2} n_p \left\{ e^{-\frac{v_s}{D} \xi} \operatorname{erfc} \left(\frac{\xi - v_s t}{\sqrt{4Dt}} \right) - \operatorname{erfc} \left(\frac{\xi + v_s t}{\sqrt{4Dt}} \right) \right\} \quad (12)$$

The erfc function decays rapidly with increasing argument, so the first erfc in the brackets of (12) is always much larger than the second (except in a small neighborhood of $t = 0$.) For most of the interesting values of v_s and D , the first term, even with the exponential factor, will dominate the expression, so we will approximate $n(x,t)$ by

$$n(x,t) \approx \frac{1}{2} n_p e^{-\frac{v_s}{D} \xi} \operatorname{erfc} \left(\frac{\xi - v_s t}{\sqrt{4Dt}} \right). \quad (13)$$

It is of interest to verify that this expression will lead to the steady-state distribution obtained earlier. As $t \rightarrow \infty$, the argument of the erfc goes to $-\infty$ for any ξ , and the erfc approaches 2. The variable ξ may be viewed as the result of a transformation from the laboratory system to a system moving with the shock, so Eq. 13 reduces to Eq. 2 in the limit as t becomes infinite. For finite values of t , however, we see that the steady-state distribution is "modulated" by the time-dependent erfc function. The form of n given by Eq. 13 is particularly convenient for describing the effect of this modulating factor, since it can be considered to be a

t-parametric description of the precursor distribution in a system of reference moving with the shock.

We can get a general idea of what to expect by examining the extremes of the dependence of the erfc on its argument. For negative values of $y < -1$, $\text{erfc}(y) \rightarrow 2$ very rapidly, while for positive values of $y > +1$, $\text{erfc}(y) \rightarrow e^{-y^2}/y\sqrt{\pi}$. This means that the precursor electron density given by Eq. 13 decays in a different way, according as $\xi \lesseqgtr v_s t$. That is

$$n(\xi, t) \rightarrow n_p e^{-\frac{v_s^2}{D}\xi}, \quad \xi < v_s t - \sqrt{4Dt} \quad (14)$$

$$n(\xi, t) \rightarrow n_p \frac{\sqrt{Dt/\pi}}{(\xi - v_s t)} e^{-\frac{(\xi + v_s t)^2}{4Dt}}, \quad \xi > v_s t + \sqrt{4Dt} \quad (15)$$

The transition between these two regimes of decay may be taken as the point for which $\xi = v_s t$, therefore the transition point is moving away from the shock front with the shock velocity v_s . In the laboratory system we have $x = 2v_s t$, so the transition point moves with twice the shock velocity. One is tempted to regard the region over which this transition takes place as a kind of "precursor front" moving ahead of the actual shock front. The width of this front can be conveniently taken as that range of ξ over which the argument of the erfc function changes from -1 to $+1$. From the conditions given in (14) and (15), this range can be written as

$$\Delta \xi = \xi_{+1} - \xi_{-1} = 4\sqrt{Dt} \quad (16)$$

It is seen that the front broadens with increasing t , and for any t is

sharper for smaller D . It will be found shortly, however, that this front is so broad as to invalidate the idea of a density "front" in the usual sense.

In order to obtain a more precise picture of this behavior, it is convenient to introduce dimensionless parameters into Eq. 13. If we write D in the alternate form, $D = v_0 L/3$, where L is the mean free path for electrons with thermal velocity v_0 in the neutral gas ahead of the shock, then the arguments of the functions in Eq. 13 may be put into the form:

$$\frac{v_s}{D} \xi = 3\rho\eta \quad , \quad \frac{(\xi - v_s t)}{\sqrt{4Dt}} = \sqrt{\frac{3\rho}{4}} \frac{(\eta - \eta')}{\sqrt{\eta'}} \quad (17)$$

with the dimensionless parameters η , η' and ρ defined by

$$\eta = \xi/L \quad , \quad \eta' = v_s t/L \quad , \quad \rho = v_s/v_0 \quad (18)$$

For medium-weight gases (argon, nitrogen, etc.), hypersonic shocks with Mach numbers of the order of 10 have velocities of about 4×10^5 cm/sec, and equilibrium temperatures of the order of 10^4 degrees Kelvin. Actually, if we assume the electron temperature to be equal to the equilibrium temperature of the gas, then for hypersonic shocks in ideal gases, v_s and v_0 are each approximately proportional to the Mach number, so the ratio $\rho = v_s/v_0$ is independent of Mach number and equal to about 6×10^{-3} . On the other hand, the mean free path, L , can differ by an order of magnitude from one gas to another, and is often a sensitive function of electron temperature. With this in mind, a reasonably informative presentation of the transient behavior

described by Eq. 13 can be obtained for an ideal gas by setting $\rho = 6 \times 10^{-3}$ and plotting $\log (n/n_p)$ against η for several values of the normalized shock front position η' . Such a family of curves is plotted in Fig. 4.

The curves in Fig. 4 fail to suggest the existence of any kind of well-defined precursor "front". The reason for this may be seen by writing the front width given in Eq. 16 in terms of the dimensionless parameters defined in (18):

$$\Delta\eta = \Delta\xi/L = 4\sqrt{v_0 t/3L} = 4\sqrt{\eta'/3\rho} \quad (19)$$

The exponent of the steady-state decay factor $e^{-3\rho\eta}$ therefore changes over the transition region by an amount

$$3\rho\Delta\eta = 4\sqrt{3\rho\eta'}$$

This means that the width of the transition region, even for very small values of t , is quite a bit greater than a decay length for the steady-state distribution, so the effect of the modulating erfc function in Eq. 13 is spread over a large part of the precursor distribution.

III. Some Implications of the Transient Behavior

Although the precursor density does not possess a well-defined front, it is possible that under suitable experimental circumstances the behavior shown in Fig. 4 could give rise to a virtual front propagating ahead of the shock. The existence of such a virtual front would depend on the nature of the

interaction of the measuring apparatus with the precursor density, and could occur under several experimental conditions. Let us list the characteristics of some probes which, if placed along the path of the shock, would imply the existence of a precursor front.

1. A probe fails to respond until the electron density reaches a certain level.
2. A probe saturates at a given electron density.
3. The response of a probe changes discontinuously at a critical electron density.

In each of these cases, the nature of the response of a probe of some sort depends critically on a certain electron density, and it is the propagation of this critical level that constitutes the advancing "front".

A.) Comparison of the theory with some experimental results.

The critical level involved in case 1 might be simply the local electron density required to bring the response of the probe above the noise level, or some other threshold, associated with the detection system. This could have been the basis of the "precursor front" observed by Weymann using induction probes.⁽¹⁾ He claims that the precursor signal had a pronounced front, but a very rapidly growing electron density rising from the detection limit of his apparatus could simulate such a front. Let us assume that this was the case, and attempt to match the propagation of a level of constant density on Fig. 4 with the x-t diagram of a measured precursor signal front. The diagram we will use is Fig. 2 of reference 1. This figure has been reproduced on Fig. 5 of this report.

The conditions under which the measured data were obtained are not provided, but they may be guessed from information given elsewhere in the paper. For example, in Fig. 3 Weymann gives formative time lags for various diaphragms bursting into either 3 or 6 mmHg of argon. The only lags as short as that in his Fig. 2 occur for pressures of 3 mmHg. Taking this as the pressure of the driven gas, we find in his Conclusions estimates of electron temperature (about 10^4 degrees K), and diffusion coefficient (about 4×10^6 cm²/sec), from which one obtains a mean free path, L , of about 0.2cm. Thus we can establish the normalized distances $\eta = \xi/L$ and $\eta' = v_s t/L$ in our Fig. 4 in terms of the measured distances in his Fig. 2. This, in turn, makes it possible to look for a level of constant density in Fig. 4 whose propagation is consistent with the signal front motion Weymann has measured.

We choose two shock front positions on Fig. 5, say $(v_s t)_1 = 43$ cm and $(v_s t)_2 = 76$ cm, and measure the distance from shock to signal front in each case. We find that the signal front has moved relative to the shock front from $\xi_1 = 62$ cm to $\xi_2 = 104$ cm, while the shock front itself has moved $(76 - 43)$ cm = 33cm. Using $L = 0.2$ cm to convert to our normalized coordinates, we get

$$\eta_1 = \xi_1/L = 310, \quad \eta_2 = \xi_2/L = 520,$$

while

$$\Delta\eta' = \Delta(v_s t)/L = 165.$$

With these data, we now enter Fig. 4 with a horizontal line whose end-points must simultaneously lie on the vertical lines $\eta_1 = 310$, $\eta_2 = 520$ and

span two decay curves for values of η'_1 and η'_2 such that $\eta'_2 - \eta'_1 = 165$. The line drawn on Fig. 4 at about $\log(n/n_p) = -11.5$ approximately satisfies this requirement by lying between $\eta'_1 = 310$ and $\eta'_2 = 520$ while spanning the decay curves for $\eta'_1 = 30$ and $\eta'_2 = 200$. The motion of a level of constant density along this line is plotted in Fig. 5 for comparison with Weymann's measurements. We see that a slightly larger formative time lag is obtained by extrapolating back to $t = 0$, and the first measured point lies below the predicted curve. However, the model assumes the instantaneous creation of an ideal shock at $t = 0$, so cannot be expected to hold very well for small values of t . The results obtained by matching at the same points for different values of L are almost identical with those shown in Fig. 5 for $L = 0.2$ cm. A larger mean free path would allow Weymann's probes to have been less sensitive.

It is of interest to observe that as $t \rightarrow \infty$, the velocity of the given density level approaches the shock velocity. This is to be expected, the transient giving way to the fixed steady-state distribution for large times. However, over the range for which the experimental data are given, we may assume that $\eta \gg \eta'$, so the approximation given in (15) can be used for the precursor density. Clearly, the exponential factor dominates the decay, so we may write

$$n(x,t) \propto e^{-\frac{x^2}{4Dt}} \quad (20)$$

where we have taken $\xi + v_s t = (x - v_s t) + v_s t = x$. If the density is to

remain constant, so must the exponent. Thus the point x at which this constant density is observed must vary with time according to

$$x \propto \sqrt{4Dt}$$

so the speed of this level in the laboratory system has the time-dependence

$$\frac{dx}{dt} \propto t^{-1/2} \quad (21)$$

One should not infer from this equation that $dx/dt \rightarrow 0$ for large t . For large t , the approximation $\eta \gg \eta'$ no longer holds, and we must find dx/dt by requiring that $dn/dt = 0$ in Eq. 13. It is easily shown that as $t \rightarrow \infty$, $dn/dt = 0$ implies $dx/dt \rightarrow v_s$ as shown in Fig. 5. Weymann concluded, presumably from several sets of measurements, that the velocity of the signal front in shock tube coordinates could be approximately represented by Eq. 21. This behavior can be verified for the motion of the level of constant density indicated on Fig. 4. The velocity of the transient "precursor front", relative to the shock front, may be written

$$\frac{d\xi}{dt} = v_s \frac{d\xi/L}{d(v_s t)/L} = v_s \frac{d\eta}{d\eta'} \quad (22)$$

therefore the velocity of the precursor front relative to the laboratory system becomes

$$\frac{dx}{dt} = v_s \left(1 + \frac{d\eta}{d\eta'} \right) \quad (23)$$

The derivative $d\eta/d\eta'$ can be estimated from Fig. 4 for various values of

η' (hence t , since $t = L\eta'/v_s$) along the line of constant density $\log(n/n_p) = -11.6$ when $L = 0.2$ cm. A plot of Eq. 23 is given in Fig. 6, along with points obtained from Weymann's empirical formula (or our Eq. 21) by normalizing the two expressions at $t = 150$ sec. The agreement over the experimental range, $t \lesssim 150$, is seen to be good, as one might expect. Our model is therefore capable of an a priori prediction of at least one qualitative feature of the experimental results.

The arguments presented here are not intended to "verify" the predictions of the simple heuristic theory developed in this report, but rather to demonstrate that these predictions are to some extent consistent with the only relevant measurements published so far. However, armed with a bit more confidence, we will go on to discuss the implications of such a transient precursor front in the scattering of electromagnetic waves.

B.) Effect of the transient on the scattering of electromagnetic waves.

If a plane electromagnetic wave is normally incident upon the shock, the presence of the precursor electrons ahead of the front can be expected to affect the scattering properties of the shock. Typically in problems of this sort, there are many parameters to be considered. Some, like the frequency of the incident wave or the density of the driven gas, may vary over wide ranges. Others, like the shock speed, the **equilibrium** gas temperature and the electron mean free paths, are not precisely known and must be estimated. Still others, like the model parameters n_p and T_p , are not known at all and must be guessed. In this section we will assume driven gas pressures of a few mmHg, equilibrium gas temperatures of about 10^4 degrees K,

and shock speeds of about 4×10^5 cm/sec. The precursor electron temperature will be taken to be equal to the temperature of the hot gas. Electron mean free paths ahead of the shock can be either small, as in air, or large, as in the noble gases, the ratio being ten or twenty to one. A reasonable guess for the model parameter n_p is very difficult to justify, and therefore requires more extended discussion.

As part of Weymann's early investigations,⁽¹⁾ he used a magnetic probe to obtain an estimate of the precursor density far ahead of the shock. He concluded, by an indirect argument, that for a Mach 12 shock in 4mmHg of argon, the precursor density is about $10^7/\text{cm}^3$ at a distance of 100 cm ahead of the shock front. Later measurements⁽⁴⁾ showed, as was mentioned in the Introduction, that the spatial dependence of the precursor distribution is given by our Eq. 1, which implies Eq. 2, from which n_p can be obtained from the measured density. Using $D = 3 \times 10^6 \text{ cm}^2/\text{sec}$ (for 4mmHg argon) and $v_s = 4 \times 10^5 \text{ cm/sec}$, we find that $n_p \approx 6 \times 10^{12}/\text{cm}^3$. This seems like a large number. If, however, the level of equilibrium ionization in this shock is calculated from the information given by Resler, et al,⁽¹⁰⁾ it is found that $n_{eq} \approx 2 \times 10^{15}/\text{cm}^3$, so n_p is several orders of magnitude below the equilibrium density behind the onset point. (It is also of interest to observe that in order to make the electron energy-exchange mechanism work in a low-voltage arc in argon at a few mmHg, Druyvesteyn found that electron densities of the order of $10^{12}/\text{cm}^3$ were required.⁽⁹⁾)

To simplify the scattering picture, let us assume that the decay length, $\delta = D/v_s$, of the steady-state precursor distribution is very much larger than

the distance from the shock front to the onset point. In virtue of the large electron densities behind the onset point, we will assume this region to be a perfect conductor, and move it up to the shock front to give the following form to the scattering obstacle:

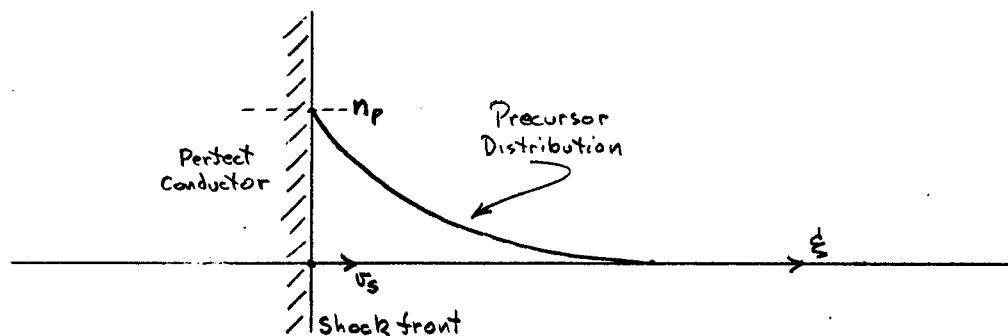


Fig. 7

There are now two characteristic numbers which determine the approximations which can be used in examining the scattering properties of the shock. One of these is the maximum plasma frequency encountered in the precursor region; this is $\omega_{p0} = (e^2 n_p / m \epsilon_0)^{1/2} \approx 2\pi \times 10^{10}$ rad/sec. The other is a characteristic wavelength equal to the decay length, from which we may define a frequency $\omega_\delta = 2\pi c/\delta$. Unfortunately, we have no idea of how n_p depends on the type or pressure of the driven gas, and the possible range ω_δ is quite large. In order to reduce confusion, let us assume that $\omega_\delta < \omega_{p0}$, which, if our various hypotheses are correct, will be the case for a Mach 10-12 shock in a few mmHg of argon. In this case the division of the frequency spectrum will look something like



Fig. 8

It should be kept in mind that we are not dealing with a stationary scattering problem. The shock is in motion, and the reflected wave carries knowledge of this motion through a time-varying phase factor. The scattering problem should properly take into account both the time and space variations of the electron distribution; an analysis in terms of the continuous frequency spectrum of the scattered wave would be appropriate. However, the shaky structure of hypothesis and inference erected thus far can hardly justify such a detailed analysis. It will be adequate for our purpose to consider the shock front fixed when calculating the effect of the precursor electrons on the incident and reflected waves. The "ether drag" associated with the motion of the precursor will give perturbations of opposite sign for the two waves, and can therefore be expected to contribute corrections of order $(v_s/c)^2$. Shock speeds being what they are, this is negligible. Accordingly, any change in the Doppler effect will be considered to arise from changes of the precursor distribution relative to the moving shock, rather than to a fixed observer.

Scattering at various frequencies below, between and above the reference points in Fig. 8 will now be discussed in a qualitative way.

1.) Low-Frequencies: $\omega \ll \omega_0$.

At these low frequencies, the steady-state precursor distribution extends only a fraction of an incident wavelength from the shock front, and may be replaced by an equivalent plane sheet of thickness δ and electron density n_p . Whatever its properties, such an electrically thin layer cannot be expected to change the reflecting properties of the region over which it is placed in any

significant way. This can easily be verified. For the transient case, the effect of a perturbation that grows in a reasonable time interval from zero to an insignificant value is still insignificant. We will conclude, then, that at sufficiently low frequencies, the electron precursor will produce no observable effects.

2.) High-Frequencies: $\omega \gg \omega_{po}$.

For sufficiently high frequencies, the scattering amplitude can be calculated in the geometrical optics approximation. Consider, for the moment, a stationary scattering problem. Assuming a time-dependence $\exp(-j\omega t)$, the electric field in the presence of a space-varying electron density $n(x)$ must satisfy the equation

$$\frac{d^2 E}{dx^2} + (k_0^2 - \beta_p^2(x))E = 0 \quad (24)$$

where

$$k_0^2 = \omega^2/c^2, \quad \beta_p^2(x) = e^2 n(x)/\epsilon_0 m c^2 (1 - j\nu_c/\omega). \quad (25)$$

Under the conditions given above, $\beta_p \ll k_0$ and $(d\beta_p^2/\beta_p^2 dx) \ll k_0$, so the conditions for the application of the geometrical optics approximation are satisfied, and we may write⁽¹¹⁾,

$$E(x) \propto e^{\pm j \int^x \sqrt{k_0^2 - \beta_p^2(x)} dx} \quad (26)$$

To avoid needless complication, it may be reasonably assumed that $\nu_c/\omega \ll 1$, making β_p^2 a real positive number.

TECHNICAL LIBRARY
U. S. ARMY CORP. HEADQUARTERS
ABERDEEN PROVING GROUND, MD.
ORDEG-TL

It will be helpful to consider first the degenerate case in which there are no precursor electrons. A reference plane (which could represent a receiving antenna) will be established at x_0 , and the shock front will be located at $x_s < x_0$, as in the figure below:

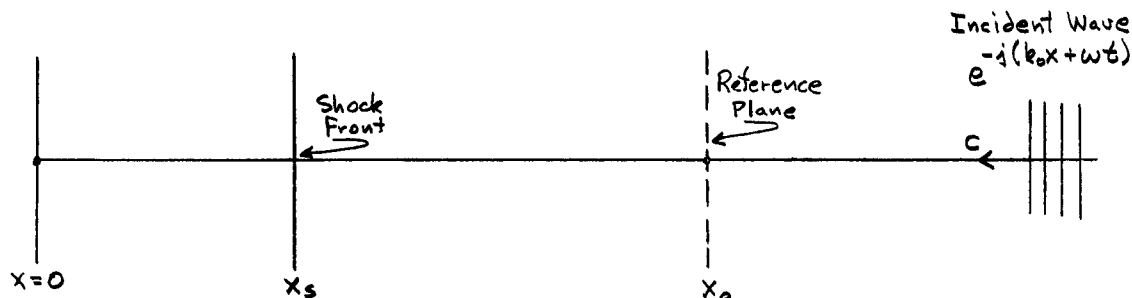


Fig. 9

The incident wave at x_0 is simply $E_{inc} = \exp(-j(k_0 x_0 + \omega t))$. But this wave moves past x_0 up to x_s , where it is reflected (phase increase of 180°) and sent back toward x_0 . Using Eq. 26 with $\beta_p^2 = 0$, we can calculate the phase accumulation factor in the round trip from x_0 to x_s to x_0 . Adding $j\pi$ to account for the reflection by a perfect conductor, and multiplying by the incident wave at x_0 , we get the reflected wave at x_0 in the form

$$E_{refl}(x_0) = -e^{2j \int_{x_s}^{x_0} k_0 dx} e^{-j(k_0 x_0 + \omega t)}, \quad (27)$$

which can be rewritten as

$$E_{refl}(x_0) = -e^{j(k_0 x_0 - \omega t - 2k_0 x_s)} \quad (28)$$

Let us now reintroduce the motion of the shock by setting $x_s = v_s t$, and define the generalized frequency of a wave at a fixed point as the time rate of change of its phase; that is,

$$\omega' = j \frac{d\Phi}{dt} \quad (29)$$

For the reflected wave given in Eq. 28, the phase is

$$\Phi = j(k_0 x_0 - \omega t - 2k_0 v_s t),$$

so its frequency is

$$\omega'_{refl} = \omega + 2k_0 v_s = \omega + 2\omega \frac{v_s}{c}, \quad (30)$$

thus displaying the Doppler shift produced by the motion of the shock.

The perturbation introduced by the steady-state precursor distribution can be calculated by writing the exponent in Eq. 26 in the approximate form

$$j \int_0^x k_0 (1 - \beta_p^2(x)/2k_0^2) dx = j \int_0^x k_0 dx - \frac{j}{2k_0} \int_0^x \beta_p^2(x) dx. \quad (31)$$

The first term contributes the phase component we have already discussed. In view of our earlier discussion, the second term is to be calculated relative to the moving shock. Therefore, transforming to the shock-based coordinates, and assuming that x_0 is sufficiently far away that $\beta_p^2(x_0) \approx 0$ for all times of interest, we may write the precursor contribution to the phase Φ as,

$$\underline{\Phi}_p = -\frac{j}{k_0} \int_{x_s}^{x_0} \beta_p^2(x) dx = -\frac{j}{k_0} \frac{\omega_{p0}^2}{c^2} \int_0^\infty e^{-\frac{v_s}{D} \xi} d\xi = -j \frac{\beta_{p0}^2}{k_0} \frac{D}{v_s}. \quad (32)$$

This is simply a fixed phase shift in the reflected wave, and could therefore contribute nothing of observable interest.

Under transient conditions, however, β_p^2 is growing from effectively zero to its steady-state value. Since the effective dielectric constant of the electron distribution is less than unity, the growth of the precursor will be accompanied by a decrease with time of the total phase. This will result in an increase in the Doppler shift inferred from the reflected wave. The time dependence of that part of the phase due to the precursor can be introduced by altering the first equality of (32) to read

$$\underline{\Phi}_p(t) = -\frac{j}{k_0} \int_0^\infty \beta_p^2(\xi, t) d\xi, \quad (33)$$

where the integration is again performed in shock coordinates. The frequency of the reflected wave now becomes

$$\omega'_{refl} = j \frac{d \underline{\Phi}_{Total}}{dt} = \omega + 2k_0 v_s + \frac{1}{k_0} \int_0^\infty \frac{\partial \beta_p^2(\xi, t)}{\partial t} d\xi \quad (34)$$

The time derivative of β_p^2 may be found by using $n(\xi, t)$ from Eq. 13. The time differentiation and subsequent ξ -integration are straightforward, though complicated, and we will record only the result:

$$\Delta \omega'_p = \frac{1}{k_0} \int_0^\infty \frac{\partial \beta_p^2(\xi, t)}{\partial t} d\xi = \frac{\beta_{p0}^2}{2k_0} \sqrt{\frac{D}{\pi t}} e^{-\frac{v_s^2 t}{4D}}. \quad (35)$$

For an upper limit of the effect produced in this way, let us calculate $\Delta\omega'_p$ for $k_0 = \beta_{po}$, $v_s = 4 \times 10^5$ cm/sec and $D = 4 \times 10^6$ cm²/sec, (the driven gas is argon at about 3mmHg.) The unperturbed Doppler shift is $\Delta\omega'_u = 2k_0 v_s$. Below is a little table showing the way in which $(\Delta\omega'_p/\Delta\omega'_u)$ behaves with increasing time.

$t(\mu\text{sec})$	$(\Delta\omega'_p/\Delta\omega'_u)$
10	0.20
20	0.13
50	0.06
100	0.026
200	0.007

We see that the perturbation here is at most a small fraction of the normal Doppler effect.

3.) Intermediate-Frequencies: $\omega_0 < \omega < \omega_{po}$.

Over a certain restricted range of frequencies, it is possible that the transient behavior of the precursor may produce a more pronounced effect than in the two extreme cases just discussed. For ω in the range given above, one can still assume that the precursor extends over several incident wavelengths ($\omega_0 < \omega$), but for some value of $\xi > 0$, the coefficient of E in Eq. 24 vanishes. This means that the effective dielectric constant of the precursor vanishes at some point ahead of the shock, and the incident wave is perfectly reflected at that point. For a given frequency ω , this point is defined by the equation

$$\beta_p^2(x_r) = k_0^2 = \omega^2/c^2,$$

or, solving for n in shock coordinates (since $x_r = x_s + \xi_r$),

$$n(\xi_r) = \epsilon_0 m \omega^2 / e^2. \quad (36)$$

In the steady-state, the incident wave is simply reflected from a point at the fixed distance ξ_r ahead of the actual shock front, and the phase of the reflected wave is changed by a fixed amount.

During the transient period of precursor accumulation, however, the point of reflection, ξ_r , moves forward from the actual shock front. That is, since this point corresponds to the critical density defined by the right side of Eq. 36, the propagation of this density level, as discussed at the beginning of the section, will produce a corresponding movement of the point of reflection. The appropriate density can be represented by a horizontal line on Fig. 4, and the velocity of the reflection point will resemble the precursor "front" velocity shown in Fig. 6. This will show up as an enhanced Doppler shift at the beginning of the shock.

We can make these observations a bit more quantitative by using the WKB approximation⁽¹¹⁾ in solving Eq. 24. We begin, as in the high-frequency case, by considering a stationary scattering problem. Taking x_0 in Fig. 9 sufficiently far away from the shock, the asymptotic form of the local turning-point solution may be used:⁽¹¹⁾

$$E(x_0) \sim \sqrt{\frac{2}{\pi k_0}} A \left[e^{j(\omega - \pi/4)} + e^{-j(\omega - \pi/4)} \right] \quad (37)$$

where

$$w = \int_{x_r}^{x_0} \sqrt{k_0^2 - \beta_p^2(x)} dx. \quad (38)$$

The constant A is to be determined by the requirement that the electric field E at x_0 be the sum of the incident wave and a reflected wave. One way to find such a constant is to add and subtract k_0 in the integrand of Eq. 38, writing w in the form

$$w = \int_{x_r}^{x_0} k_0 dx - \int_{x_r}^{x_0} f(x) dx = k_0(x_0 - x_r) - \int_{x_r}^{x_0} f(x) dx \quad (39)$$

where

$$f(x) = [k_0 - \sqrt{k_0^2 - \beta_p^2(x)}]. \quad (40)$$

Reintroducing the time dependence $\exp(-j\omega t)$ into Eq. 37, we obtain,

$$E(x_0, t) = E(x_0) e^{-j\omega t} = \sqrt{\frac{2}{\pi k_0}} A \left[e^{j k_0 x_0 - j k_0 x_r - j \int_{x_r}^{x_0} f(x) dx - j \frac{\pi}{4} - j\omega t} \right. \\ \left. + e^{-j k_0 x_0 + j k_0 x_r + j \int_{x_r}^{x_0} f(x) dx + j \frac{\pi}{4} - j\omega t} \right]. \quad (41)$$

The incident wave at x_0 must be $\exp(-j(k_0 x_0 + \omega t))$, and can be identified in the second term in the brackets above. We choose A in such a way that the incident wave is left standing alone, by taking

$$A = \sqrt{\frac{\pi k_0}{2}} e^{-j k_0 x_r - j \int_{x_r}^{x_0} f(x) dx - j \frac{\pi}{4}} \quad (42)$$

This accomplishes the required decomposition of $E(x_0, t)$:

$$E(x_0, t) = e^{-j(k_0 x_0 + \omega t)} + \left\{ -j e^{-j 2 k_0 x_r - j 2 \int_{x_r}^{x_0} f(x) dx} \right\} e^{+j(k_0 x_0 - \omega t)} \quad (43)$$

The reflection coefficient is the expression in brackets. Having isolated the reflected wave, the various terms in its phase will now be recombined, giving

$$\Phi_{\text{refl}}(t) = -j \left(k_0 x_0 + \omega t - 2 \int_{x_r}^{x_0} \sqrt{k_0^2 - \beta_p^2(x, t)} dx \right). \quad (44)$$

The integral in this equation extends from the reflection (or turning) point x_r to the far-removed observation point x_0 . Accordingly, β_p^2 is different from zero over only a small part of the range of integration, and a reasonable approximation can be expected if we simply ignore β_p^2 and write

$$\int_{x_r}^{x_0} \sqrt{k_0^2 - \beta_p^2} dx \approx k_0 (x_0 - x_r). \quad (45)$$

Equation 44 then becomes

$$\Phi_{\text{refl}}(t) \approx -j \left[-k_0 x_0 + \omega t + 2 k_0 (v_s t + \xi_r(t)) \right], \quad (46)$$

where we have written $x_r = x_s + \xi_r(t) = v_s t + \xi_r(t)$. According to (29), the frequency of the reflected wave becomes

$$\omega'_{\text{refl}} \approx \omega + 2 k_0 v_s + 2 k_0 \frac{d \xi_r(t)}{dt}. \quad (47)$$

The time dependence of $\xi_r(t)$ is most easily obtained by reference to Fig. 4. A given frequency ω defines an electron density through Eq. 36, and thus a horizontal line on Fig. 4. The velocity of propagation of this level relative to the shock front can then be found numerically in terms of increments $d\eta$ and $d\eta'$. (See Eq. 22 and the discussion following it.)

If the electron density upstream of the reflection point is taken into account in (45), the effect is to produce a slight additional time varying decrease in the phase. This will augment the Doppler effect still further, since the smaller the phase, the closer the reflection point appears to be to the observation point x_0 . We will not bother with this small effect, other than to observe that as a result, the approximation (47) is a lower limit to the enhanced Doppler shift.

The magnitude of the shift will depend upon the size of ω compared to ω_{p0} . The value of n_p inferred from Weymann's measurements is $n_p \approx 6 \times 10^{12}/\text{cm}^3$, so let us be as optimistic as possible and assume that such a value is not unrealistic. If we take a few representative frequencies, 2 kmc, 5 kmc and 8 kmc, we find the critical densities defined by Eq. 36 are $8.3 \times 10^{-3} n_p$, $5.2 \times 10^{-2} n_p$ and $0.13 n_p$, respectively. These numbers define the dotted horizontal lines shown on Fig. 4. The effective shock velocity, inferred from the Doppler shift of the reflected wave, can be estimated from Eq. 23 for each of these frequencies. The results are plotted in Fig. 10 as v_{eff} vs. t , where the driven gas is again 3 mmHg argon. We see that the lower the frequency, the greater the effect. It should be remembered, however, that the WKB approximation requires that the electron density should not decay too rapidly over an incident wavelength. In fact, this is already violated for the lower frequencies in the

example above.

It is unlikely that any of the effects discussed here could be observed in air, the main reason being that the ratio v_s/D is so much larger in air than in an ideal gas like argon. The equilibrium temperature of the shock heated gas will be less for air than for an ideal gas at the same shock speed. More important, the collision probability for electrons at the usual shock temperatures is more than an order of magnitude greater in air. This means that the mean free path is so small that any transient effects that might occur, can have a duration of only a few microseconds. For example, in Fig. 6, the reduction of mean free path by a factor 1/10 will divide the t-scale by 10 and everything would be over after about $15 \mu\text{sec}$. Moreover, the approximation on which Fig. 10 is based would be completely invalid, since D/v_s would now be only about 1 cm, while the shortest incident wavelength is almost 4 cm.

IV. Summary and Conclusions

How much confidence can be placed in the electron diffusion hypothesis underlying the results obtained here? The answer to this question is related, in part, to the results themselves. Actual electrons, as well as electrical effects allegedly due to them, have been detected far ahead of shock fronts, and the most compelling explanation for these observations is that the electrons got there by diffusion. This hypothesis is immediately called into question by a vague expectation that strong space-charge fields would prohibit any appre-

ciable charge separation. But without an adequate theory of this admittedly complex physical situation, there is no more reason to reject than to accept the diffusion hypothesis. We have attempted to give credence to the idea of electron diffusion through the shock front by suggesting a few mechanisms that are thought to operate in different, but somehow analogous, situations. In the end, we are led to accept the hypothesis, at least provisionally, and to ask what its implications might be, and whether these implications are consistent with the existing experimental data. The model we have chosen to study is heuristic, in the sense that it emphasizes the particular features of the hypothesis we wish to examine, and leads to fairly clear predictions of behavior which can be measured. Comparing these predictions with the data already available, we discover the following:

- 1.) The spatial dependence of the predicted steady-state electron distribution agrees with both the elementary theory and the measured results.
- 2.) The transient behavior of the precursor distribution obtained from the model suggests the possibility of observing a "precursor front" under certain conditions. Allowing a reasonable interpretation of the way in which the observed precursor front was measured, it is found that the predictions of the model are consistent with the experimental results. In fact, the empirical time-dependence of the observed precursor front velocity is given exactly.

Furthermore,

- 3.) It is suggested that the transient should produce a relatively pro-

nounced effect on the scattering of electromagnetic waves in a certain frequency range, (for suitable gases and pressures.)

An experiment is being planned to check this behavior.

In short, these results have added a few more pieces to the pattern of plausible inference which presently supports the electron diffusion hypothesis. If the scattering experiment mentioned above should prove successful, further supporting evidence would be provided.

Theory and experiment agree that the dramatic precursor effects are to be found in the noble gases. For shocks in air, the lower gas temperatures and much smaller mean free paths combine to limit sharply both the spatial range of the precursor distribution and the duration of the transient. However, experiments using the noble gases are likely to provide additional information about the electrical characteristics of the shock front region.

REFERENCES

1. H. D. Weymann, "Electron Diffusion Ahead of Shock Waves in Argon", Phys. Fluids, 3, 545 (1960).
2. P. Gloersen, "Some Unexpected Results of Shock-Heating Xenon", Phys. Fluids, 3, 857 (1960).
3. F. Schultz-Grunow, Unpublished work described at a Brown University Engineering Colloquium, Dec., 1960.
4. H. D. Weymann and B. Troy, "Electron and Ion Density Profiles Ahead of Shock Waves in Argon", Bull. Am. Phys. Soc., Series II, Vol. 6, No. 2, p. 212, March 20, 1961.
5. R. G. Fowler, G. W. Paxton and H. G. Hughes, "Electrons as a Shock Driver Gas", Phys. Fluids, 4, 234 (1961).
6. R. G. Fowler and B. D. Fried, "Theory of Electron Driven Shock Waves", Phys. Fluids, 4, 767 (1961).
7. H. Petschek and S. Byron, "Approach to Equilibrium Ionization behind Strong Shock Waves in Argon", Ann. Phys., 1, 270 (1957).
8. W. P. Allis and D. J. Rose, "Transition from Free to Ambipolar Diffusion", Phys. Rev., 93, 84 (1954).
9. M. J. Druyvesteyn, "Der Niedervoltbogen", Z. Physik, 64, 781 (1930).
10. E. L. Resler, S. C. Lin and A. Kantrowitz, "The Production of High Temperature Gases in Shock Tubes", J. Appl. Phys., 33, 1390 (1952).
11. P. M. Morse and H. Feshbach, "Methods of Theoretical Physics", (McGraw-Hill, New York, 1953), Chapt. 9.

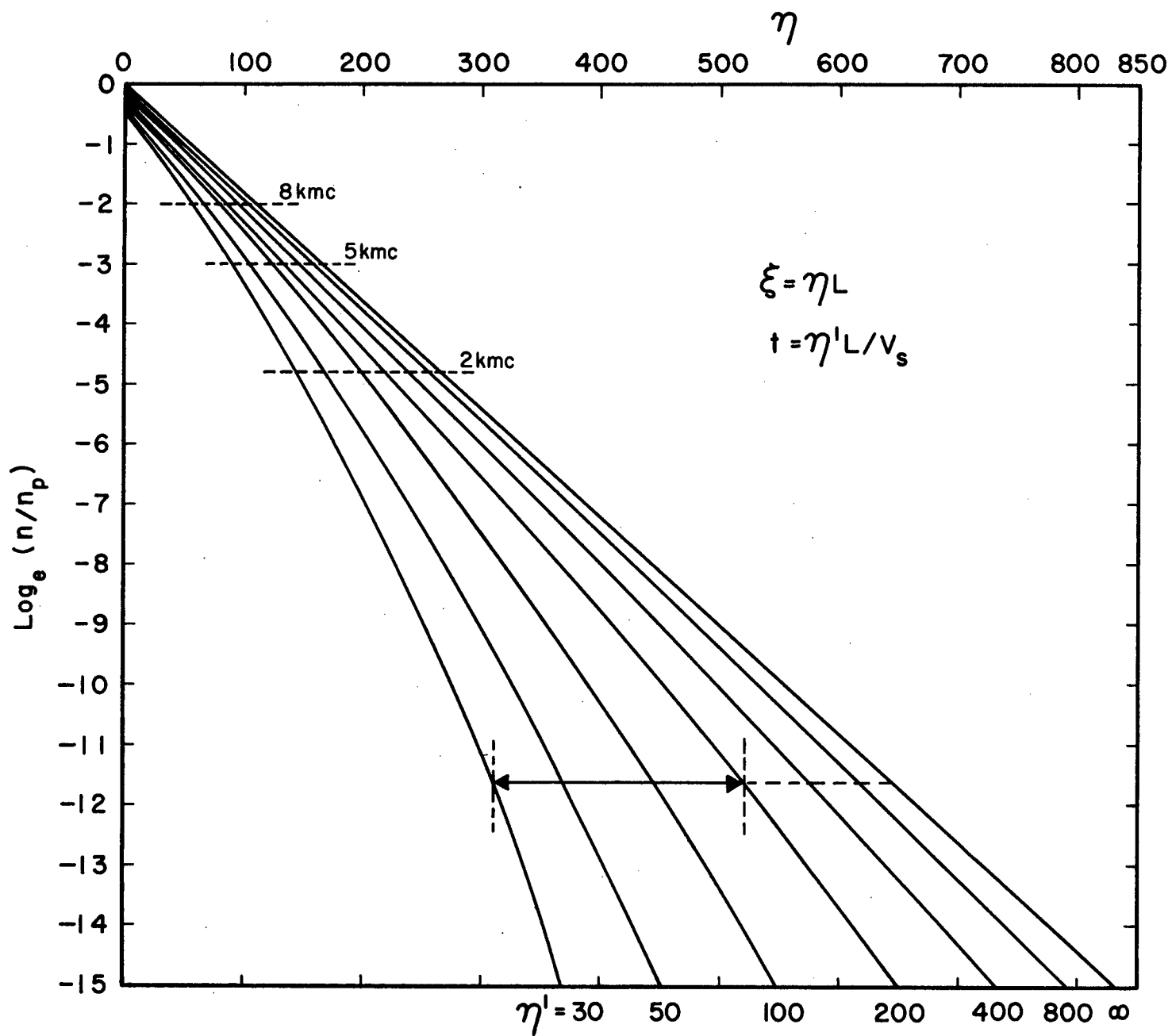


FIG. 4 BEHAVIOR OF PRECURSOR ELECTRON DENSITY AS A FUNCTION OF ξ AND t . ($\rho = V_s / V_0 = 6 \times 10^{-3}$)

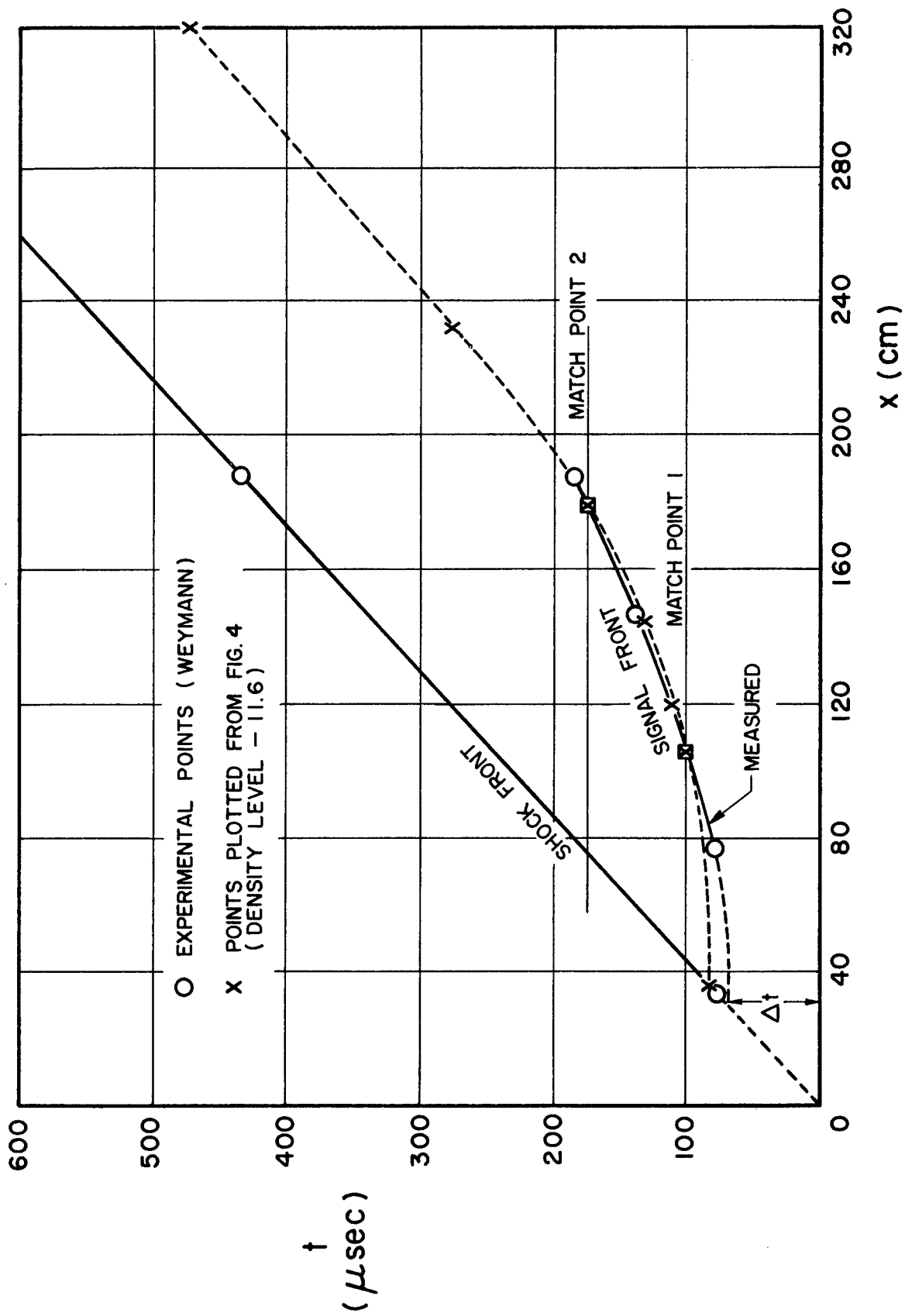


FIG. 5 COMPARISON OF MEASURED SIGNAL FRONT WITH THAT OBTAINED FROM FIG. 4

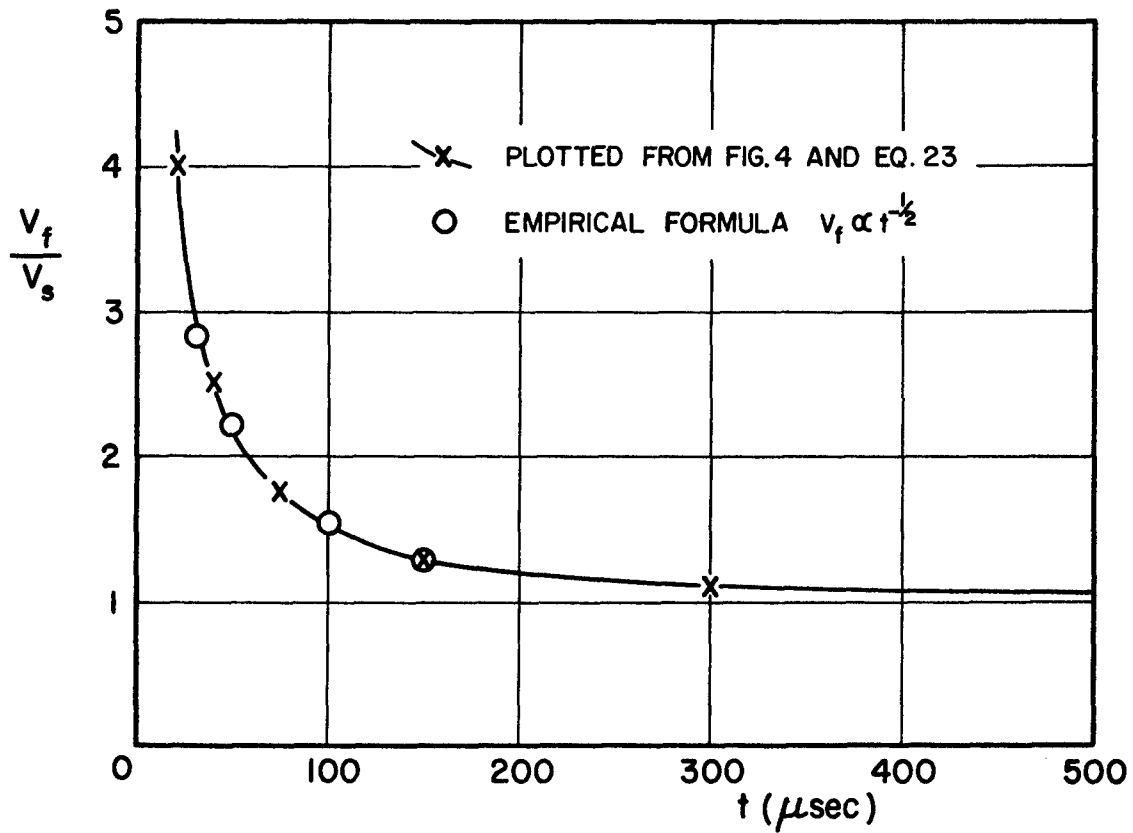


FIG. 6 COMPARISON OF PREDICTED AND EMPIRICAL SIGNAL FRONT VELOCITIES

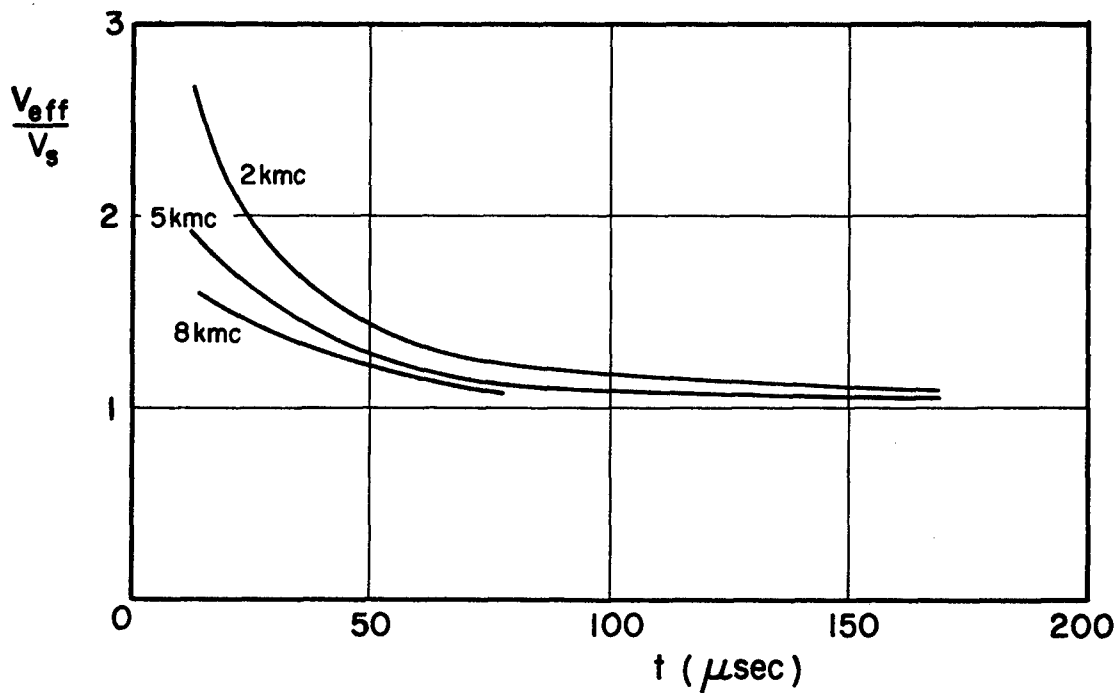


FIG. 10 EFFECTIVE SHOCK VELOCITY FROM DOPPLER SHIFT FOR FREQUENCIES 2 kmc, 5 kmc, 8 kmc.

LIST S-S

<u>Code</u>	<u>Organization</u>	<u>No. of Copies</u>
AF 29	APGC (PGTRI, Tech Library) Eglin AFB Florida	1
AF 124	RADC (RCOIL-2) Griffiss AFB New York	1
AF 139	AF Missile Dev. Cen. (MDGRT) Attn: Technical Library Holloman AFB New Mexico	1
AF 18	AUL Maxwell AFB Alabama	1
AF 5	AF Missile Test Cen. Patrick AFB Florida Attn: AFMTC, Tech Library, MU-135	1
AF 227	USAF Security Service (CLR) San Antonio, Texas	1
AF 28	Hq. USAF (Major R. L. Stell) Tactical Air Group Washington 25, D.C.	1
AF 91	AFOSR (SRY, Technical Director) 14th Street and Constitution Avenue Washington, D.C.	1
AF 166	Hq. USAF (AFOAC-S/E) Communications-Electronics Directorate Washington 25, D.C.	1
AF 314	Director of Air Force Research Division AFRD Washington, D.C.	1
AF 63	WADD (WCLRSA, Mr. Portune) Wright-Patterson AFB Ohio	

<u>Code</u>	<u>Organization</u>	<u>No. of Copies</u>
AF 43	ASD (ASAPRL) Wright-Patterson AFB Ohio	1
AF 68	ASD (ASRNRE-3) Attn: Mr. Paul Springer Wright-Patterson AFB Ohio	1
AF 231	Director, Electronics Division Air Technical Intelligence Center Attn: AFCIN-4E1, Colonel H. K. Gilbert Wright-Patterson AFB Ohio	1
AF 308	WADD (WDRTR, Mr. A. D. Clark) Directorate of System Engineering Dyna Soar Engineering Office Wright-Patterson AFB Ohio	1
Ar 42	Director U. S. Army Ordnance Ballistic Research Laboratories Aberdeen Proving Ground Maryland Attn: Ballistic Measurements Laboratory	1
Ar 47	Ballistic Research Laboratories Aberdeen Proving Ground Maryland Attn: Technical Information Branch	1
Ar 3	Director Evans Signal Laboratory Belmar, New Jersey Attn: Mr. O. C. Woodyard	1
Ar 5	U. S. Army Signal Engineering Laboratories Evans Signal Laboratory Belmar, New Jersey Attn: Technical Document Center	1

<u>Code</u>	<u>Organization</u>	<u>No. of Copies</u>
AF 253	EOARDC Shell Building 47 Rue Cantersteen Brussels, Belgium	1
Ar 78	Commanding General, SIGFM/EL-PC U. S. Army Signal Engineering Labs. Fort Monmouth, New Jersey Attn: Dr. Horst H. Kedesdy Deputy Chief, Chem-Physics Branch	1
Ar 49	Commanding General U. S. Army Signal Engineering Labs. Fort Monmouth, New Jersey Attn: SIGFM/EL-AT	1
Ar 39	Commander USASRDL Fort Monmouth, New Jersey Attn: Mr. F. J. Triola	1
Ar 67	Commander Army Rocket & Guided Missile Agency Redstone Arsenal Alabama Attn: Technical Library, ORDXR-OTL	4
Ar 9	Chief of Research & Development Department of the Army Washington 25, D.C. Attn: Scientific Information Branch	1
Ar 41	Office of Chief Signal Officer Engineering & Technical Division Washington 25, D.C. Attn: SIGNET-5	1
G 59	Advisory Group on Electric Parts Room 103, Moore School Building 200 South 33rd Street Philadelphia 4, Pennsylvania	1
G 2	ASTIA Arlington Hall Station Arlington 12, Virginia	10

<u>Code</u>	<u>Organization</u>	<u>No. of Copies</u>
G 103	National Aeronautical Space Agency Langley Aeronautical Research Laboratory Langley, Virginia Attn: Mr. Cliff Nelson	1
G 8	Library National Bureau of Standards Boulder Laboratories Boulder, Colorado	2
G 13	National Bureau of Standards U. S. Department of Commerce Washington 25, D. C. Attn: Mr. A. G. McNish	1
G 27	National Bureau of Standards U. S. Department of Commerce Washington 25, D.C. Attn: Gustave Shapiro, Chief Engineering Electronics Section Electricity and Electronics Division	1
G 49	Director National Security Agency Washington 25, D.C. Attn: R/D (331)	7
G 6	Office of Technical Services Department of Commerce Washington 25, D.C. Attn: Technical Reports Section	2
M 6	AFCRL, Office of Aerospace Research (CRREL) L. G. Hanscom Field Bedford, Massachusetts	10
M 17	AFCRL, Office of Aerospace Research (CRRD) Attn: Carlyle J. Sletten L. G. Hanscom Field Bedford, Massachusetts	3
	AFCRL, Office of Aerospace Research (CRRD) Attn: Contract Files L. G. Hanscom Field Bedford, Massachusetts	2

<u>Code</u>	<u>Organization</u>	<u>No. of Copies</u>
M 54	Hq. AFCCDD (CCRRC, Capt, John J. Hobson) L. G. Hanscom Field Bedford, Massachusetts	1
M 59	AFCCDD L. G. Hanscom Field Bedford, Massachusetts	1
G 116	NASA (Dr. R. V. Hess) NASA Langley Research Center Hampton, Virginia	1
N 1	Director, Avionics Division (AV) Bureau of Aeronautics Department of the Navy Washington 25, D.C.	1
N 16	Commander U. S. Naval Air Missile Test Center Point Mugu, California Attn: Code 366	1
N 27	Librarian U. S. Naval Postgraduate School Monterey, California	1
N 29	Director U. S. Naval Research Laboratory Washington 25, D.C. Attn: Code 2027	2
N 30	Dr. J. I. Bohnert, Code 5210 U. S. Naval Research Laboratory Washington 25, D.C.	1
N 37	Chief of Naval Research Department of the Navy Washington 25, D.C. Attn: Code 427	1

<u>Code</u>	<u>Organization</u>	<u>No. of Copies</u>
N 48	Commanding Officer U. S. Haval Air Development Center Johnsville, Pennsylvania Attn: NADC Library	1
N 85	Commanding Officer and Director U. S. Navy Electronics Laboratory (Library) San Diego 52, California	1
N 86	Chief, Bureau of Ordnance Department of the Navy Surface Guided Missile Branch Washington 25, D.C. Attn: Code ReS1-e	1
N 88	Department of the Navy Bureau of Aeronautics Technical Data Division, Code 4106 Washington 25, D.C.	1
N 91	Commander U. S. Naval Air Test Center Patuxent River, Maryland Attn: ET-315, Antenna Branch	1
N 141	ARDC Regional Office c/o Department of the Navy Room 4549, Munitions Building Washington 25, D.C.	1
N 73	Office of Naval Research Branch Office, London Navy 100, Box 39 F. P. O. New York, New York	10
I 1	Airborne Instruments Laboratory, Inc. Division of Cutler Hammer Walt Whitman Road Melville, L. I. New York Attn: Library	1
I 388	Aircom Inc. 354 Main Street Winthrop, Massachusetts	1

<u>Code</u>	<u>Organization</u>	<u>No. of Copies</u>
I 374	ACF Industries, Inc. Southeast Corner, 52nd Avenue and Jackson Street Bladensburg, Prince George's County Maryland Attn: Librarian	1
I 205	Battelle Memorial Institute 505 King Avenue Columbus 1, Ohio Attn: Wayne E. Rife, Project Leader Electrical Engineering Division	1
I 8	Bell Aircraft Corporation Post Office Box One Buffalo 5, New York Attn: Eunice P. Hazelton, Librarian	1
I 469	Bell Telephone Laboratories Murray Hill New Jersey	1
I 13	Bell Telephone Laboratories, Inc. Whippany Laboratory Whippany, New Jersey Attn: Technical Information Library	1
I 940	Aerospace Corp. Box 95085 Los Angeles 45, California Attn: Library	1
I 247	Bendix Radio Division Bendix Aviation Corporation E. Joppa Road Towson 4, Maryland Attn: Dr. D. M. Allison, Jr. Director Engineering & Research	1
I 248	Bjorksten Research Laboratories, Inc. P. O. Box 265 Madison, Wisconsin Attn: Librarian	1

<u>Code</u>	<u>Organization</u>	<u>No. of Copies</u>
I 25	Cornell Aeronautical Laboratory, Inc. 4455 Genesee Street Buffalo 21, New York Attn: Librarian	1
I 255	Dalmo Victor Company A Division of Textron, Inc. 1515 Industrial Way Belmont, California Attn: Mary Ellen Addems, Technical Librarian	1
I 28	Dorne and Margolin, Inc. 29 New York Avenue Westbury, Long Island, New York	1
I 257	Douglas Aircraft Co., Inc. 827 Lapham Street El Segundo, California Attn: Engineering Library	1
I 258	Douglas Aircraft Company, Inc. 3000 Ocean Park Boulevard Santa Monica, California Attn: Peter Duyan, Jr. Chief, Electrical/Electronics Section	1
I 259	Douglas Aircraft Company, Inc. 2000 North Memorial Drive Tulsa, Oklahoma Attn: Engineering Librarian, D-250	1
I 187	Electromagnetic Research Corporation 5001 College Avenue College Park, Maryland Attn: Mr. Martin Katzin	1
I 415	Electronica Communication 1830 York Road Timonium, Maryland	1

<u>Code</u>	<u>Organization</u>	<u>No. of Copies</u>
I 299	Electronic Specialty Company 5121 San Fernando Road Los Angeles 39, California Attn: Donald L. Margerum Chief Engineer, Radiating Systems Division	1
I 262	Emerson Electric Mfg. Co. 8100 West Florissant Avenue St. Louis 21, Missouri Attn: Mr. E. R. Breslin, Librarian	1
I 147	Emerson Radio-Phonograph Corp. Emerson Research Laboratories 701 Lamont Street, N.W. Washington 10, D.C. Attn: Mrs. R. Corbin, Librarian	1
I 264	Fairchild Aircraft-Missiles Division Fairchild Eng. and Airplane Corp. Hagerstown, Maryland Attn: Library	1
I 266	Federal Telecommunication Laboratories 500 Washington Avenue Nutley 10, New Jersey Attn: Technical Library	1
I 269	General Electric Company Electronics Park Syrcause, New York Attn: Documents Library B. Fletcher, Building 3-143A	1
I 793	General Electric Company Missile and Space Vehicle Department 3198 Chestnut Street Philadelphia, Pennsylvania Attn: Documents Library	1
I 893	General Electric Company 3750 D Street Philadelphia 24, Pennsylvania Attn: Mr. H. G. Lew Missile and Space Vehicle Department	1

<u>Code</u>	<u>Organization</u>	<u>No. of Copies</u>
I 270	General Precision Laboratory, Inc. 63 Bedford Road Pleasantville, New York Attn: Librarian	1
I 48	Goodyear Aircraft Corp. 1210 Massillon Road Akron 15, Ohio Attn: Library, Plant G	1
I 448	Granger Associates Electronic Systems 974 Commercial Street Palo Alto, California Attn: John V. N. Granger, President	1
I 737-	The Hallicrafters Co. 5th and Kostner Avenues Chicago 24, Illinois Attn: Henri Hodara, Head of Space Communication	1
I 207	Hughes Aircraft Company Antenna Department Building 12, Mail Station 2714 Culver City, California Attn: Dr. W. H. Kummer	1
I 56	Hughes Aircraft Company Florence Ave. and Teale Streets Culver City, California Attn: Louis L. Bailin Manager, Antenna Department	1
I 265	ITT Laboratories 3700 East Pontiac Street Fort Wayne 1, Indiana Attn: Technical Library	1
I 230	Jansky and Bailey, Inc. 1339 Wisconsin Avenue, N.W. Washington 7, D.C. Attn: Mr. Delmer C. Ports	1

<u>Code</u>	<u>Organization</u>	<u>No. of Copies</u>
I 241	Dr. Henry Jasik, Consulting Engineer 298 Shames Drive Brush Hollow Industrial Park Westbury, New York	1
I 279	Lockheed Aircraft Corporation 2555 N. Hollywood Way California Division Engineering Library Department 72-25, Plant A-1, Building 63-1 Burbank, California Attn: N. C. Harnois	1
I 468	Lockheed Aircraft Corporation Missile Systems Division Research Library Box 504, Sunnyvale, California Attn: Miss Eva Lou Robertson, Chief Librarian	1
I 136	The Martin Company P. O. Box 179 Denver 1, Colorado Attn: Mr. Jack McCormick	1
I 280	The Martin Company Baltimore 3, Maryland Attn: Engineering Library Antenna Design Group	1
I 282	McDonnell Aircraft Corporation, Dept. 664 Box 516 St. Louis 66, Missouri Attn: C. E. Zoller Engineering Library	1
I 116	Melpar, Inc. 3000 Arlington Boulevard Falls Church, Virginia Attn: Engineering Technical Library	1
I 648	The Mitre Corporation 244 Wood Street Lexington 73, Massachusetts Attn: Mrs. Jean E. Claflin, Librarian	1

<u>Code</u>	<u>Organization</u>	<u>No. of Copies</u>
I 934	Motorola, Inc. Phoenix Research Laboratory 3102 N. 56th Street Phoenix, Arizona Attn: Dr. A. L. Aden	1
I 641	National Research Council Radio & Electrical Engineering Division Ottawa, Ontario, Canada Attn: Dr. G. A. Miller, Head Microwave Section	1
I 284	North American Aviation, Inc. 12214 Lakewood Boulevard Downey, California Attn: Technical Information Center (495-12) Space and Information Systems Division	1
I 285	North American Aviation, Inc. Los Angeles International Airport Los Angeles 45, California Attn: Engineering Technical File	1
I 82	Northrop Corporation Norair Division 1001 E. Broadway Hawthorne, California Attn: Mr. E. A. Freitas, Library Dept. 3145	1
I 286	Page Communications Engineers, Inc. 2001 Wisconsin Avenue, N.W. Washington 7, D.C. Attn: (Mrs.) Ruth Temple, Librarian	1
I 287	Philco Corporation C and Tioga Streets Philadelphia 34, Pennsylvania Attn: Mrs. Dorothy B. Collins Research Librarian	1
I 225	Pickard and Burns, Inc. 240 Highland Avenue Needham 94, Massachusetts Attn: Dr. Richard H. Woodward	1

<u>Code</u>	<u>Organization</u>	<u>No. of Copies</u>
I 288	Polytechnic Research & Development Co. Inc. 202 Tillary Street Brooklyn 1, New York Attn: Technical Library	1
I 232	Radiation Engineering Laboratory Main Street Maynard, Massachusetts Attn: Dr. John Ruze	1
I 289	Radiation, Inc. P. O. Drawer 37 Melbourne, Florida Attn: Technical Library, Mr. M. L. Cox	1
I 914	Radiation Systems, Inc. 440 Swann Avenue Alexandria, Virginia Attn: Library	1
I 290	RCA Laboratories David Sarnoff Research Center Princeton, New Jersey Attn: Miss Fern Cloak, Librarian	1
I 291	Radio Corporation of America Defense Electronic Products Building 10, Floor 7 Camden 2, New Jersey Attn: Mr. Harold J. Schrader, Staff Engineer Organization of Chief Technical Administrator	1
I 757	Radio Corporation of America Surface Communications Systems Laboratory 75 Varick Street New York 13, New York Attn: Mr. S. Krevsky	1
I 789	Radio Corporation of America West Coast Missile and Surface Radar Division Engineering Library, Building 306/2 Attn: L. R. Hund, Librarian 8500 Balboa Boulevard Van Nuys, California	1

<u>Code</u>	<u>Organization</u>	<u>No. of Copies</u>
I 930	Radio Corporation of America Defense Electronic Products Advanced Military Systems Princeton, New Jersey Attn: Mr. David Shore	1
I 292	Director, USAF Project RAND Via: AF Liaison Office The Rand Corporation 1700 Main Street Santa Monica, California	1
I 547	The Rand Corporation 1700 Main Street Santa Monica, California Attn: Technical Library	1
I 373	Rantec Corporation 23999 Ventura Boulevard Calabasas, California Attn: Grace Keener, Office Manager	1
I 294	Raytheon Company Wayland Laboratory Wayland, Massachusetts Attn: Miss Alice G. Anderson, Librarian	1
I 472	Raytheon Company Missile Systems Division Hartwell Road Bedford, Massachusetts Attn: Donald H. Archer	1
I 295	Republic Aviation Corporation Farmingdale, Long Island, New York Attn: Engineering Library	1
I 142	Sanders Associates, Inc. 95 Canal Street Nashua, New Hampshire Attn: Mr. Norman R. Wild	1

<u>Code</u>	<u>Organization</u>	<u>No. of Copies</u>
I 96	Sandia Corporation, Sandia Base P. O. Box 5800 Albuquerque, New Mexico Attn: Classified Document Division	1
I 546	Sandia Corporation Attn: Organization 1423 Sandia Base Albuquerque, New Mexico	1
I 682	Scanwell Laboratories, Inc. 6601 Scanwell Lane Springfield, Virginia	1
I 312	Space Technology Laboratories, Inc. P. O. Box 95001 Los Angeles 45, California Attn: Technical Information Center Document Procurement	1
I 297	Sperry Gyroscope Company Great Neck, Long Island, New York Attn: Florence W. Turnbull Engineering Librarian	1
I 367	Stanford Research Institute Documents Center Menlo Park, California Attn: Acquisitions	1
I 104	Sylvania Electric Products, Inc. 100 First Avenue Waltham 54, Massachusetts Attn: Charles A. Thornhill, Report Librarian Waltham Laboratories Library	1
I 818	Sylvania Reconnaissance Systems Lab. Box 188 Mountain View, California Attn: Marvin D. Waldman	1

<u>Code</u>	<u>Organization</u>	<u>No. of Copies</u>
I 240	TRG, Inc. 2 Aerial Way Syosset, New York Attn: M. L. Henderson, Librarian	1
I 338	A. S. Thomas, Inc. 355 Providence Highway Westwood, Massachusetts Attn: A. S. Thomas, President	1
I 708	Texas Instruments, Inc. 6000 Lemmon Avenue Dallas 9, Texas Attn: John B. Travis Systems Planning Branch	1
I 139	Westinghouse Electric Corp. Electronics Division Friendship Int'l Airport Box 1897 Baltimore 3, Maryland Attn: Engineering Library	1
U 61	Brown University Department of Electrical Engineering Providence, Rhode Island Attn: Dr. C. M. Angulo	1
U 157	California Institute of Technology Jet Propulsion Laboratory 4800 Oak Grove Drive Pasadena, California Attn: Mr. I. E. Newlan	1
U 99	California Institute of Technology 1201 E. California Street Pasadena, California Attn: Dr. C. Papas	1
U 3	Space Sciences Laboratory Leuschner Observatory University of California Berkeley 4, California Attn: Dr. Samuel Silver, Professor of Engineering Science and Director, Space Sciences Laboratory	1

<u>Code</u>	<u>Organization</u>	<u>No. of Copies</u>
U 100	University of California Electronics Research Lab. 332 Cory Hall Berkeley 4, California Attn: J. R. Whinnery	1
U 289	University of Southern California University Park Los Angeles, California Attn: Dr. Raymond L. Chuan Director, Engineering Center	1
U 239	Case Institute of Technology Electrical Engineering Department 10900 Euclid Avenue Cleveland, Ohio Attn: Professor Robert Flonsey	1
U 183	Columbia University Department of Electrical Engineering Morningside Heights, New York, New York Attn: Dr. Schlesinger	1
U 238	University of Southern California University Park Los Angeles 7, California Attn: Z. A. Kaprielian Associate Professor of Electrical Engineering	1
U 10	Cornell University School of Electrical Engineering Ithaca, New York Attn: Professor G. C. Dalman	1
U 86	University of Florida Department of Electrical Engineering Gainesville, Florida Attn: Professor M. H. Latour, Library	1

<u>Code</u>	<u>Organization</u>	<u>No. of Copies</u>
U 59	Library Georgia Technology Research Institute Engineering Experiment Station 722 Cherry Street, N.W. Atlanta, Georgia Attn: Mrs. J. H. Crosland, Librarian	1
U 102	Harvard University Technical Reports Collection Gordon McKay Library 303 Pierce Hall Oxford Street Cambridge 38, Massachusetts Attn: Librarian	1
U 103	University of Illinois Documents Division Library Urbana, Illinois	1
U 104	University of Illinois College of Engineering Urbana, Illinois Attn: Dr. P. E. Mayes, Department of Electrical Engineering	1
U 169	Illinois Institute of Technology 3301 S. Dearborn Street Chicago 16, Illinois Attn: Dr. George I. Cohn	1
U 240	Illinois Institute of Technology Technology Center Department of Electrical Engineering Chicago 16, Illinois Attn: Paul C. Yuen Electronics Research Laboratory	1
U 22	The John Hopkins University Homewood Campus Baltimore 18, Maryland Attn: Dr. Donald E. Kerr Department of Physics	1

<u>Code</u>	<u>Organization</u>	<u>No. of Copies</u>
U 105	The John Hopkins University Applied Physics Laboratory 8621 Georgia Avenue Silver Spring, Maryland Attn: Mr. George L. Seielstad	1
U 228	University of Kansas Electrical Engineering Department Lawrence, Kansas Attn: Dr. H. Unz	1
U 68	Lowell Technological Institute Research Foundation P. O. Box 709 Lowell, Massachusetts Attn: Dr. Charles R. Mingins	1
U 32	Massachusetts Institute of Technology Research Laboratory of Electronics Building 26, Room 327 Cambridge 39, Massachusetts Attn: John H. Hewitt	1
U 26	Massachusetts Institute of Technology Lincoln Laboratory P. O. Box 73 Lexington 73, Massachusetts Attn: Mary A. Granese, Librarian	1
U 34	McGill University Montreal, Canada Attn: Professor G. A. Woonton Director, The Eaton Electronics Research Laboratory	1
U 107	University of Michigan Electronic Defense Group Engineering Research Institute Ann Arbor, Michigan Attn: J. A. Boyd, Supervisor	1
U 37	University of Michigan Engineering Research Institute Willow Run Laboratories, Willow Run Airport Ypsilanti, Michigan Attn: Librarian	1

<u>Code</u>	<u>Organization</u>	<u>No. of Copies</u>
U 108	University of Minnesota Minneapolis 14, Minnesota Attn: Mr. Robert H. Stumm, Library	1
U 194	Physical Science Laboratory New Mexico College of Agriculture and Mechanic Arts State College, New Mexico Attn: Mr. H. W. Haas	1
U 39	New York University Institute of Mathematical Sciences Room 802, 25 Waverly Place New York 3, New York Attn: Professor Morris Kline	1
U 96	Northwestern University Microwave Laboratories Evanston, Illinois Attn: R. E. Beam	1
U 78	Ohio State University Research Foundation 1314 Kinnear Road Columbus 8, Ohio Attn: Dr. T. E. Tice Department of Electrical Engineering	1
U 109	The University of Oklahoma Research Institute Norman, Oklahoma Attn: Professor C. L. Farrar, Chairman Electrical Engineering	1
U 45	The Pennsylvania State University Department of Electrical Engineering University Park, Pennsylvania	1
U 185	University of Pennsylvania Institute of Cooperative Research 3400 Walnut Street Philadelphia, Pennsylvania Attn: Department of Electrical Engineering	1

<u>Code</u>	<u>Organization</u>	<u>No. of Copies</u>
U 48	Polytechnic Institute of Brooklyn Microwave Research Institute 55 Johnson Street Brooklyn, New York Attn: Dr. Arthur A. Oliner	1
U 97	Polytechnic Institute of Brooklyn Microwave Research Institute 55 Johnson Street Brooklyn, New York Attn: Mr. A. E. Laemmel	1
U 184	Purdue University Department of Electrical Engineering Lafayette, Indiana Attn: Dr. Schultz	1
U 176	Stanford University W. W. Hasen Laboratory of Physics Stanford, California Attn: Microwave Library	1
U 110	Syracuse University Research Institute Collendale Campus Syracuse 10, New York Attn: Dr. C. S. Grove, Jr. Director of Engineering Research	1
U 309	Technical University Oestervoldgade 10 G Copenhagen, Denmark Attn: Professor Hans Lottrup Knudsen	1
U 186	University of Tennessee Ferris Hall W. Cumberland Avenue Knoxville 16, Tennessee	1
U 111	The University of Texas Electrical Engineering Research Lab. P. O. Box 8026 University Station Atustin 12, Texas Attn: Mr. John R. Gerhardt, Assistant Diector	1

<u>Code</u>	<u>Organization</u>	<u>No. of Copies</u>
U 51	The University of Texas Defense Research Laboratory Austin, Texas Attn: Claude W. Horton, Physics Library	1
U 132	University of Toronto Department of Electrical Engr. Toronto, Canada Attn: Professor G. Sinclair	1
U 133	University of Washington Department of Electrical Engineering Seattle 5, Washington Attn: G. Held, Associate Professor	1
U 187	University of Wisconsin Department of Electrical Engineering Madison, Wisconsin Attn: Dr. Scheibe	1